Towards a numerical simulation of a closed loop pulsating heat pipe in different gravity levels

M Manzoni[1,6], M Mameli[1], C de Falco[2], L Araneo[3], S Filippeschi[4], M Marengo[1,5]

[1] University of Bergamo, Engineering Department, Viale Marconi 5, 24044 Dalmine (BG), Italy
[2] Politecnico di Milano, MOX-Modeling and Scientific Computing, Mathematics Department, Piazza Leonardo da Vinci 32, 20133 Milano, Italy
[3] Politecnico di Milano, Energy Department, Via Lambruschini 4A, 20158 Milano, Italy
[4] University of Pisa, DESTEC, Largo Lazzarino 2, 56122 Pisa, Italy
[5] University of Brighton, School of Computing, Engineering and Mathematics, Lewes Road, BN2 4GJ, Brighton, UK

[6] Corresponding author, miriam.manzoni@unibg.it

Abstract. A Closed Loop Pulsating Heat Pipe (CLPHP) is a new concept of wickless heat pipe, which represents a promising and a flexible solution for moderately high heat flux applications. Numerous are the attempts to simulate the complex behaviour of a CLPHP and in particular one model was already successfully implemented by two of the authors (Mameli and Marengo). However, none of the existing models is able to well represent the effects of various gravity levels, and therefore a novel lumped parameter numerical model for the transient thermo-hydraulic simulation of a CLPHP has been developed. It consists of a two-phase separated flow model applicable to a confined operating regime, meaning that capillary slug flow is assumed a priori. A complete set of balance ordinary differential equations (mass, momentum and energy) accounts for thermal and fluid-dynamic phenomena. The suppression of the common assumption of saturated vapor plugs and the consequent implantation of heterogeneous phase changes represent the principal novelties with respect to the previous codes. The numerical tool is here used to simulate the thermal-hydraulic behavior of a planar CLPHP made of a copper tube (I.D./O.D. 1.1mm/2.0mm) and partially filled with FC-72 in modified gravity conditions (1g, 2g and 10g). This simulated configuration has already been tested experimentally both on ground (normal gravity) and on the ESA-ESTEC Large Diameter Centrifuge which allows reaching accelerations up to 20g. First comparisons with these operating conditions are provided.

Keywords: Two-phase flow, Pulsating Heat Pipe, Numerical model, Gravity force

1. Introduction

The present industry demand of high heat transfer capability coupled with relatively cheaper component leads to the evolution of novel two-phase passive devices. The Closed Loop Pulsating Heat Pipe (CLPHP) is a new concept of wickless heat pipe and represents a promising and a flexible solution suitable for moderately high heat flux applications (up to 30 W/cm^2) [1].

Patented by Akachi [2, 3], it consists of a small tube closed end-to-end in a loop, evacuated and partially filled with a working fluid, with alternated heating and cooling zones. If the tube has capillary dimension, the fluid distributes itself inside it as a train of liquid slugs and vapor plugs, which are surrounded by a thin liquid film (figure 1). Despite its relatively simple structure, the PHP thermal-hydraulic behavior is complex. Basically, when heating power is provided to the evaporator section, the pressure inside the vapor bubbles located in this region increases: vapor expands pushing the adjacent liquid toward the condenser zone where heat is rejected to a cold source and condensation possibly occurs. This leads to oscillation and circulation of the fluid within the device. Furthermore, other forces, like gravity, may act assisting or damping the fluid motion.
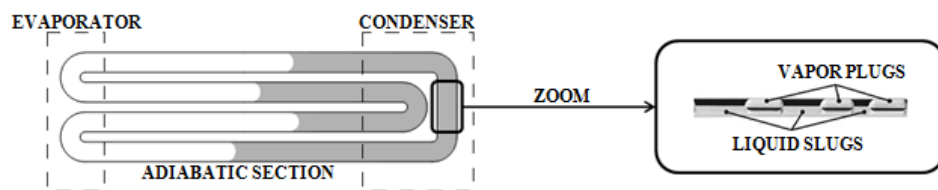
Figure 1. Schematic of a CLPHP.

In the last two decades many studies have been conducted aiming at the prediction of the actual performance of a PHP, but only few of them are capable of a complete thermal-hydraulic simulation and are even partially validated against experimental data [4,5]. Moreover none of these models are able to well represent the effects of various gravity levels.

Two of the most comprehensive numerical studies have been conducted by Holley and Faghri [6] in 2005 and by Nikolayev [7] in 2011. Holley and Faghri proposed a one dimensional lumped parameter model of a CLPHP working with water. Slug flow and saturated conditions were assumed. Momentum equation was solved for each liquid slug, while energy equation for both phases and for the external wall. The number of fluidic elements was allowed to vary during the whole simulation time due to liquid coalescence and new vapor formation. This model was subsequently improved by Mameli et al. [8,9] taking into account the effects of the local pressure losses due to the presence of turns and implementing a non-homogeneous heat transfer approach. Furthermore, an extended library of possible working fluid was included. Nikolayev, on the other hand, used an object-oriented method and updated Das's evaporation/condensation model [10] to deal with an arbitrary number of turns and fluidic elements. This code is able to take into account different phenomena which occurs within a PHP (e.g. liquid coalescence, film merger or rupture) and to capture some of the experimental observed flow patterns, but still need to implement the tube wall domain and to focus on the wall-to-fluid heat transfer issue.

The present work proposes a novel one dimensional lumped parameters model for the transient thermo-hydraulic simulation of a CLPHP. The model is inspired by the work of Holley and Faghri, but the modifications introduced by Mameli et al. are taken into account. It consists of a two-phase separated flow model applicable to a confined operating regime. A complete set of balance ordinary differential equations (mass, momentum and energy) accounts for thermal and fluid-dynamic phenomena. The suppression of the common assumption of saturated vapor plugs and the consequent implantation of heterogeneous phase changes represent the main novelties with respect to the previous codes.

This numerical tool is here used to simulate the performance of a planar CLPHP filled with FC-72 in modified gravity conditions. First experimental comparisons are also provided.

2. Numerical model

The present analysis has been performed with a one dimensional numerical model applicable to a confined operating regime, meaning that capillary slug flow is assumed a priori.

The global domain is the PHP tube, which is considered as a single straight channel of constant diameter where the entrance section is set equal to the exit section. The fluid control volumes follow the liquid slugs and the vapour bubbles in their oscillations and circulation within the channel (Lagrangian approach); liquid slugs and vapour plugs are, therefore, spatially traceable during the whole simulation time. Liquid slugs are subdivided into smaller domains with the same velocity but, eventually, different temperatures. The solid domain, representing the tube wall, is fixed in time (Eulerian approach). It is subdivided into smaller domains with different temperatures. Figure 2 shows a schematic visualization of the different numerical domains.
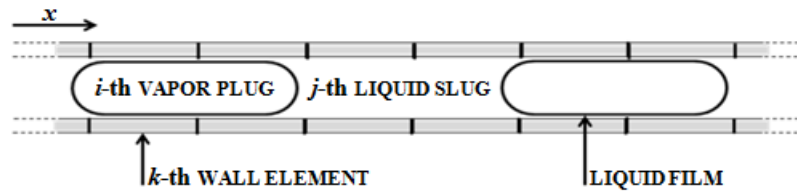
Figure 2. Schematic visualization of the numerical domains.

Code main assumptions are:
1. The model is one-dimensional. Mass, momentum and heat transfer are calculated along the axial direction, which follows the PHP tube. Heat transfer in radial direction is lumped.
2. All the fluid thermo-physical properties, apart from vapor pressure and density, are calculated as function of the temperature only. The liquid slug pressure is set equal to the average value of the adjacent vapor plugs pressure.
3. The momentum equation for each liquid slug is lumped and advection term, as well as friction between vapor plugs and wall elements, is neglected.
4. Liquid menisci maintain spherical shape with zero contact angle at the wall.
5. Vapor is treated as real gas. Density is calculated by definition (mass over volume) while Van der Waals equation is used to defined the vapor pressure as function of temperature and density.
6. Vapor may exist both in saturated (equilibrium) and not saturated conditions.
7. The thin liquid film around each vapor plug is constant in space and time and it is not considered in the definition of the heat transfer coefficients.
8. Homogeneous phase changes are neglected.

2.1. Phase changes
Although the total mass of the system remains constant during the simulation time, the mass of single liquid and vapor elements eventually varies due to phase change. Since vapor may exist both in saturated and not saturated conditions (Assumption 6 above), both heterogeneous and homogenous phase changes may take place.

Heterogonous condensation/evaporation can occur when a vapor/liquid comes into contact with an object, such a surface, that has a temperature respectively below/higher than the fluid temperature.

This involves heat transfer to/from the solid wall. In this condition, phase changes take place according to figure 3: if vapor pressure exceeds the saturation value or its temperature is lower than the saturation one, then condensation occurs; on the other hand, if liquid pressure is lower than the saturation value or its temperature overcomes the saturation one, then evaporation occurs.

2.1.1. Code implementation

Because of Assumption 8, only heterogeneous phase changes are taken into account. A combined pressure and temperature check must be done in order to assert if heterogeneous evaporation/condensation effectively occurs (figure 3). Evaporated and condensed mass is then calculated as follows:

$$m_{LV} = \int_0^{\Delta t*} \frac{A_{lat} q_{w-f}}{h_{LV}} dt \qquad if \begin{cases} T \leq T_w - \Delta T_{super-heat} \rightarrow evaporation \\ T \geq T_w + \Delta T_{cooling} \rightarrow condensation \end{cases} \tag{1}$$

$\Delta t*$ is a characteristic time associated to new liquid slugs/vapor plugs generation. A new element is, indeed, produced only if $m_{LV} \geq m_{min}$, otherwise mass exchange between adjacent elements occurs; $\Delta t*$ is proportional to the evaporation/condensation ratio at steady state and the tuning parameter, m_{min}, which allows to set the total number of fluidic elements near reasonable values.

$$\Delta t* = (m_{min}) \left(\frac{A_{lat} q_{w-f}}{h_{LV}} \right)^{-1} \tag{2}$$

For the present operative conditions, evaporative m_{min} has been set to $20\left(\frac{4}{3} \pi d_{in}^3 \rho_V\right)$ and the estimated $\Delta t*$ is 1E-2 sec, while condensed m_{min} has been set to $\frac{4}{3} \pi d_{in}^3 \rho_L$ and $\Delta t*$ is 1 sec.
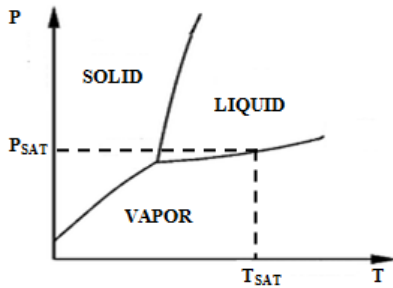
Figure 3. Phase diagram of a PHP working fluid
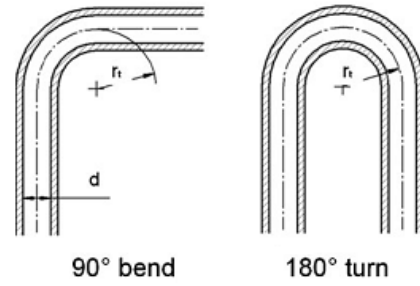
Figure 4. Geometry of 90° bend and 180° turn in the PHP.

If m_{LV} exceeds the mass of the corresponding element, then this one vanishes and the adjacent slugs/plugs merge.

2.2. Momentum equation

Taking into account Assumption 3, the momentum equation applied to the *j*-th liquid slug and integrated along its length is:

$$\left. \frac{d(mv)}{dt} \right|_j = mg \sin(\vartheta)|_j + A_{cr}(P_i - P_{i+1}) + 0.5 f_\tau \frac{m}{d} v^2 \tag{3}$$

The first term on the right side is the gravity force and ϑ is the local angle between the gravity vector and the flow direction; the second and the third terms are, otherwise, the forces respectively due to adjacent vapor expansion/compression and to viscous shear and minor losses. Due to Assumption 4 and to the constant cross section along the tube length, pressure drop due to capillary forces has been neglected.

Viscous shear is treated semi-empirically. The friction coefficient is evaluated either for fully developed laminar (Hagen-Poiseuille) o turbulent flow (Haaland equation):

$$f_\tau = \frac{64}{Re} \qquad\qquad\qquad Re < 2000$$

$$\frac{1}{\sqrt{f_\tau}} = -1.81 \log_{10}\left[\left(\frac{\varepsilon}{3.7d}\right)^{1.11} + \frac{6.9}{Re} \right] \qquad Re \geq 2000 \tag{4}$$

Minor losses are evaluated if the j-th liquid slug passes through at least a turn or a bend (figure 4). The corresponding friction coefficient is evaluated according to Darby 3K method which empirical parameters are listed in table 1:

$$f_\tau = \frac{K_{\mathrm{Re}}}{\mathrm{Re}} + K_r \left[1 + K_d \left(\frac{0.0254}{d} \right)^{0.3} \right] \quad (5)$$

Table 1. 3K constant for loss coefficient for bends and turns according to Darby.

Fitting type	r_t / d	K_{Re}	K_r	K_d
Bend 90°	1.25	800	0.091	4
Turn 180°	1.25	1000	0.1	4

By solving the momentum equation, it is possible to evaluate the velocity of each liquid slug. Their new position is, instead, calculated as:

$$x_{j,t} = x_{j,t-1} + v_j \Delta t + \frac{a_j}{2} \Delta t^2 \quad (6)$$

where a_j is the acceleration calculated as the ration between the forces applied on the j-th liquid slug and its mass.

If the spacing between two adjacent fluidic elements is zero or if there is overlap, they merges and the total number of plugs/slugs is reduced.

2.3. Energy balance

Fluid and wall temperatures are calculated accounting for the energy balance applied individually to the wall sub-domains, to each vapor plug and to each liquid slug sub-domain. The wall and the fluid energy equations are coupled with appropriate heat transfer coefficients.

The fluid energy balance is described by the following equations:

$$\frac{D(TmC_v)}{Dt} = (q_{w-f} A_{lat} - m_{LV} h_{LV}) + \left(kA_{cr} \frac{\partial T}{\partial x}\bigg|_f - kA_{cr} \frac{\partial T}{\partial x}\bigg|_b \right) - P \frac{dV}{dt} \quad (7a)$$

$$\frac{D(TmC_v)}{Dt} = mC_v \frac{\partial(T)}{\partial t} + T \frac{\partial(mC_v)}{\partial t} + v \frac{\partial(TmC_v)}{\partial x} \quad (7b)$$

The second term on the right side of equation 7a accounts for the sensible heat transferred between the wall and the fluid; the third and the last terms are respectively the axial conduction within the fluid and the compression work which is calculated only for vapor plugs. The advection term of equation 7b has been neglected and the temporal variation of the thermal capacity has been set to zero for numerical stability reasons.

The wall energy balance is, instead, defined as:

$$mC_v \frac{dT}{dt} = q_{ex} A_{ex} + \left(kA_w \frac{\partial T}{\partial x}\bigg|_f - kA_w \frac{\partial T}{\partial x}\bigg|_b \right) - q_{w-f} A_{lat} \quad (8)$$

The first term on the right side accounts for the heat exchanged between the wall and the external environment. Constant heat input flux is supplied to the evaporator zone, while forced convection is applied at the condenser. External air is considered at constant temperature T_∞. No heat exchange occurs between the wall and the environment in the adiabatic region.

$$q_{ex} = \begin{cases} Q_{ex}/A_{ex} & evaporator \\ 0 & adiabatic \\ h_\infty (T_w - T_\infty) & condenser \end{cases} \quad (9)$$

2.3.1. Heat transfer between the wall and the fluid

Both sensible and latent heat is exchanged between the wall and the fluid. Sensible heat transfer occurs by conduction and convection with laminar or turbulent flow, while phase changes comprise latent heat. Different equations have been used to estimate the heat transfer coefficient for sensible heating. The Shah and London correlation has been implemented for the laminar flow thermally developing region ($\text{Re} \leq 2000$):

$$h = \begin{cases} 1.953 \dfrac{k}{d}\left(\text{Re}\,\text{Pr}\,\dfrac{d}{L_x}\right)^{\frac{1}{3}} & \left(\text{Re}\,\text{Pr}\,\dfrac{d}{L_x}\right) \geq 33.3 \\[4mm] \dfrac{k}{d}\left(4.364 + 0.0722\,\text{Re}\,\text{Pr}\,\dfrac{d}{L_x}\right) & \left(\text{Re}\,\text{Pr}\,\dfrac{d}{L_x}\right) < 33.3 \end{cases} \tag{10}$$

where L_x is the thermal entry length and it is set equal to the evaporator/condenser length. For the transient/turbulent flow ($2000 < \text{Re} < 10000$), the Gnielinski correlation has been used:

$$h = \frac{k}{d}\left[\frac{(f_\tau/8)(\text{Re}-1E3)\text{Pr}}{1+12.7(f_\tau/8)^{1/2}\left(\text{Pr}^{2/3}-1\right)}\right] \tag{11}$$

Finally, for the fully developed turbulent flow ($\text{Re} \geq 10000$), Dittus-Boelter correlation has been applied:

$$h = 0.023\frac{k}{d}\text{Re}^{0.8}\,\text{Pr}^n \tag{12}$$

n is set to 0.4 if wall temperature is higher than fluid temperature, 0.3 otherwise.

Regarding phase change phenomena, constant heat transfer coefficients have been assumed as an initial hypothesis and these are treated as tuning parameters. For the conditions hereby analyzed they have been set as:

$$h = \begin{cases} 2000 & \dfrac{W}{m^2 K} & \textit{condensation} \\[4mm] 4000 & \dfrac{W}{m^2 K} & \textit{evaporation} \end{cases} \tag{13}$$

The above values are just a first attempt, but they are chosen in the ranges of two-phase heat transfer coefficients detected in the literature [11].

3. Model Validation

The simulated configuration has been experimentally tested in vertical position (bottom heated mode) on ground (normal gravity) and on the ESA-ESTEC Large Diameter Centrifuge [12,13] (hyper-gravity conditions).

3.1. Experimental set-up

The basic PHP structure consists of a copper tube (D.I. 1.1mm/D.O. 2.0mm) folded so as to obtain 32 parallel channels. Geometrical information are shown in figure 5. The device is evacuated and filled with FC-72 (0.5±0.03 volumetric filling ratio).

The PHP heater consists of 4 electric resistors connected in parallel (*Thermocoax® Single core 1 Nc Ac),* wrapped around the evaporator bends. Electric power is provided by a power supply (GWInstek® 3610A). The condenser section is embedded into an heat sink and cooled by means of air fans system (ebmpapst.co.uk® 8412N/2GH-214).

A pressure transducer (Kulite®, ETL/T 312, 1.2bar A) is located at the condenser section. The PHP is, also, equipped with 14 *T* type thermocouples (wire diameter 0.127mm, accuracy of ±0.1°C after calibration) located as shown in figure 5. The sensors and the power supply are connected to a data

acquisition system (NI-cRIO-9073, NI-9214®) and all signals are recorded at 16Hz. Note that despite the nine evaporator TCs are not exactly located in the heater section but just above it because of the presence of the electrical wire, these temperatures are referred in the text as evaporator temperatures.
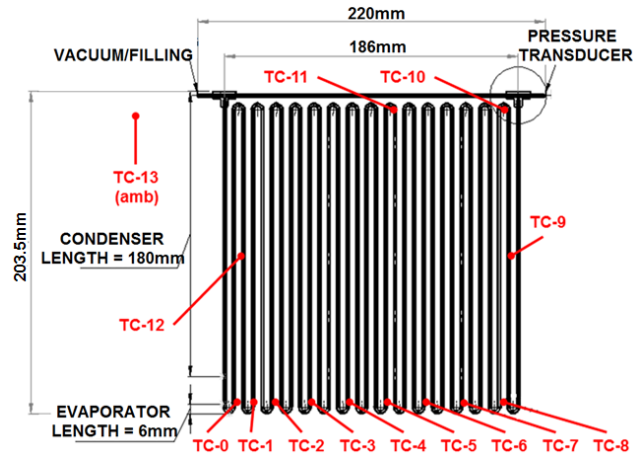
Figure 5. Technical sketch of the PHP.

3.2. Results

The numerical results have been compared with the data obtained during the ground test shown in figure 6 both in term of mean evaporator and condenser temperatures and condenser pressure. The graphs underline that, after a start-up period of about 180s, the tested device reaches a pseudo-steady state (all the temperature signals show an average value constant in time).
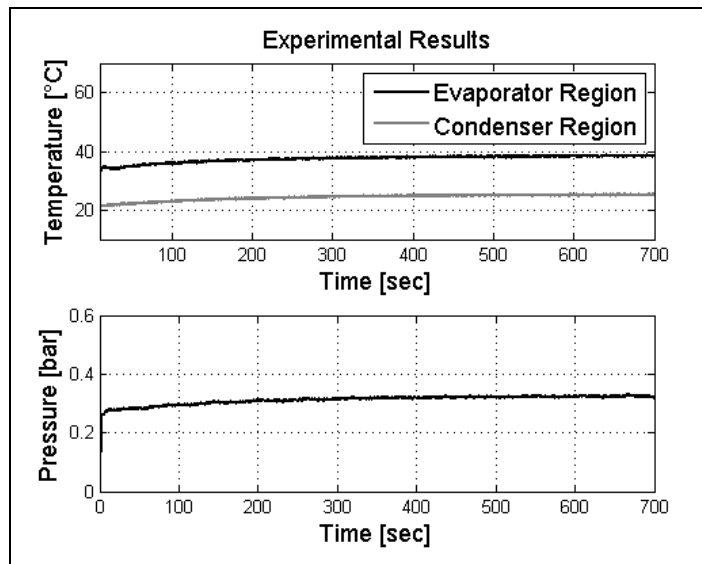
Figure 6. Ground test results: thermocouples mean temperature and condenser pressure.

Table 2. Code input parameters.

Input parameter	Value
Working fluid	FC-72
Tube material	Copper
Internal diameter	1.1 mm
External diameter	2 mm
Surface roughness	50 μm
Evaporator length	6 mm
Condenser length	180 mm
Filling ratio	0.5
Gravity acceleration	1g, 2g, 10g
Ambient temperature	20 °C
External HTC	300 W/m^{2}K
Heat power	50 W
ΔT super-heat	2.5 °C
ΔT cooling	0.1 °C
N° of wall grids	430
Time step	0.001 sec

The main input parameters of the numerical model are listed in table 2 while Figure 7 shows the predicted temperature and pressure trends.
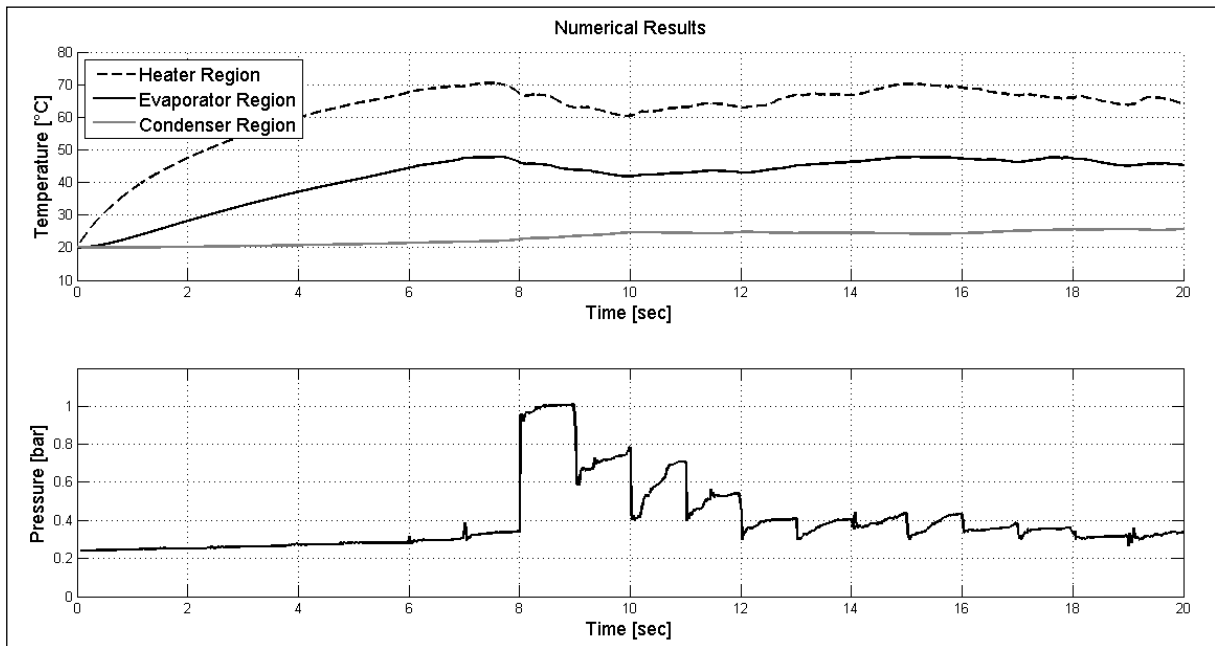
Figure 7. Numerical results: mean temperature and mean vapor pressure.

Although the code cannot reproduce the PHP transient time, principally because of the peripheral elements thermal inertia, which is not yet modeled, and a possible over estimation of the cooling medium heat transfer coefficient, the pseudo-steady state values, both in term of temperature (evaporator/condenser regions) and pressure, are close to the ones experimentally observed. The error in the evaporator temperature prediction is less than 10°C, while it reduces to negligible values for the condenser section. The evaporator temperature overestimation could be ascribed both to numerical (e.g. model simplifications, tuning values) and experimental reasons (e.g. not perfect insulation of the evaporator zone).

The lack of a homogeneous condensation model explains the overestimation of the vapor pressure. Moreover it must be taken into account that the pressure sensor is not flush mounted inside the PHP tube, but it is plugged in a T junction outside the condenser section (figure 5) damping the pressure.

Comparisons have also been made with hyper-gravity experiments performed on the ESA LDC. Figure 8 shows the mean temperature trend in the evaporator region for different gravity levels keeping the heat input constant at 50W [13]. The graph clearly shows an improvement of the device performance when gravity passes from 1g to 2g, while a deterioration appears when acceleration reaches 10g. Figure 9 otherwise shows a comparison of the predicted evaporator temperatures for 1g, 2g and 10g. Although the code is able to simulate the temperature reduction at 2g, it cannot properly predict the deep worsening at 10g. This is probably due to an overestimation of the vapor pressure especially in the evaporator region, which leads to an overrate of the fluid motion within the channel whit a consequent enhancement of the whole PHP performance. In order to improve the prediction of evaporator vapor pressure, homogeneous phase changes, in particular condensation, must be modeled. Homogeneous condensation, indeed, occurs in the fluidic bulk if the vapor pressure is higher than the saturation pressure at its actual temperature, but differently from heterogeneous phase changes no heat transfer to an external surface is required. In this case the latent heat released from the phase change involves only the fluidic element. In a bottom-heated mode PHP, for example, homogeneous condensation may occur in the evaporator region where vapor pressure may exceed the saturation one because of the acting forces, in particular gravity. In the same region, instead, heterogeneous condensation plausibly cannot occur because the wall temperature is higher than the vapor one.
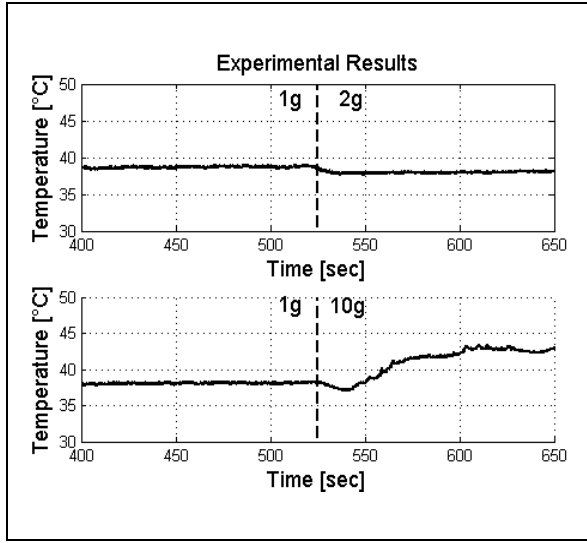
Figure 8. LDC results: mean evaporator temperature for 50W and different g-levels.
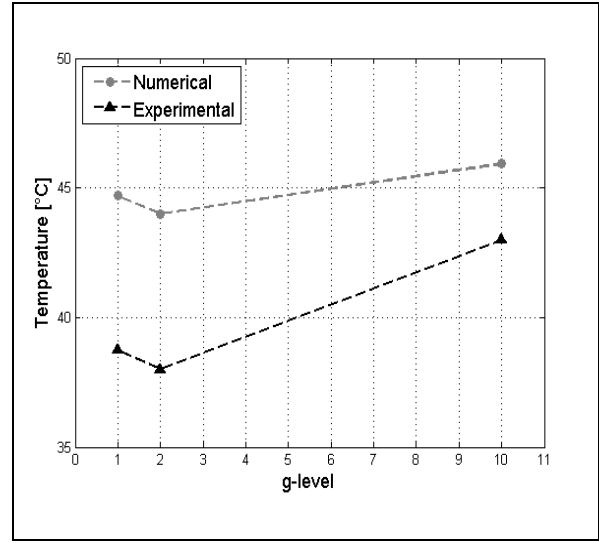
Figure 9. Mean evaporator temperature at steady state for 50W and different g-levels.

4. Conclusions

A novel one dimensional lumped parameters numerical model for the transient thermo-hydraulic simulation of a CLPHP has been developed and heterogeneous phase changes have been embedded. The comparison of the predicted results with the experimental data has shown good qualitative agreement: the maximum error in the prediction of the evaporator region temperature is, indeed, less then 10°C both at 1g and 2g and can be improved by means of a further refinement in the code. Simulations performed at higher gravity levels (10g), however, underline the need of additional improvements for the model, suggesting, in particular, the implementation of homogeneous evaporation and condensation.

Nomenclature

A_{cr}	Cross flow area, [m^2]		P	Pressure, [Pa]
A_{ext}	External lateral area, [m^2]		Pr	Prandtl number, []
A_{lat}	Lateral area, [m^2]		Q_{ex}	External heat power, [W]
A_w	Cross wall area, [m^2]		q_{ex}	External heat flux, [Wm^{-2}]
a	Acceleration, [ms^{-2}]		q_{w-f}	Heat flux between wall and fluid, [Wm^{-2}]
C_V	Specific heat constant volume, [Jkg^{-1}K^{-1}]		Re	Reynolds number, []
d	Diameter, [m]		T	Fluid temperature, [K]
f_r	Friction coefficient, []		T_w	Wall temperature, [K]
g	Gravity acceleration, [ms^{-2}]		T_∞	Environment temperature, [K]
h	Internal convection coefficient, [Wm^{-2}K^{-1}]		t	Time, [s]
h_∞	External convection coefficient, [Wm^{-2}K^{-1}]		v	Velocity, [ms^{-1}]
h_{LV}	Latent heat of vaporization, [Jkg^{-1}]		x	Axial coordinates, [m]
k	Thermal conductivity, [Wm^{-1}K^{-1}]			
m	Mass, [kg]		ε	Surface roughness, [m]
m_{LV}	Evaporated/Condensed mass, [kg]		ϑ	Inclination to horizontal, [rad]

References
[1]   Khandekar S and Groll M 2008 Roadmap to realistic modeling of closed loop pulsating heat pipes *Proc. of the 9th Int. Heat Pipe Symposium (Kuala, Malaysia, 27 June 2008)*
[2]   Akachi H, 1990 *US Patent* No. 4921041
[3]   Akachi H, 1993 *US Patent* No. 5219020
[4]   Zhang Y and Faghri A 2008 Advances and unsulved issues in pulsating heat pipes *Heat Transfer Engineering* **29** 20-44
[5]   Tang X, Sha L, Zhang H and Ju Y 2013 A review of recent experimental investigations and theoretical analyses for pulsating heat pipes *Front. Energy* **7** 161-173
[6]   Holley B and Faghri A 2005 Analysis of pulsating heat pipes with capillary wick and varying channel diameter *Int. J. Heat Mass Transfer* **48** 2635-2651
[7]   Nikolayev V S 2011 A dynamic film model of the pulsating heat pipe *J. Heat Transfer* **133** 081504
[8]   Mameli M, Marengo M and Zinna S 2012 Thermal simulation of a pulsating heat pipe: effects of different liquid properties on a simple geometry *Heat Transfer Engineering* **33** 1177-1187
[9]   Mameli M, Marengo M and Zinna S 2012 Numerical model of a multi-turn closed loop pulsating heat pipe: effect of the local pressure losses due to meanderings *Int. J. Heat Mass Transfer* **55** 1036-1047
[10]   Das S P, Nikolayev VS, Lefevre F, Pottier B, Khandekar S and Bonjour J 2010 Thermally induced two-phase oscillating flow inside a capillary tube *Int. J. Heat Mass Transfer* **53** 3905-3913
[11]   Mameli M, Marengo M, Khandekar S 2014 Local heat transfer measurement and thermo-fluid characterization of a pulsating heat pipe, *Int. J. of Thermal Sciences* **45** 140-152.
[12]   Van Loon J J W A, Krouse J, Kunha U, Goncalves J, Almeida H and Schiller P 2008 The Large Diameter Centrifuge, LDC, for Life and Physical Sciences and Technology *Proc. of the Life in Space for Life on Earth Symposium (Angers, France, 22-27 June 2008)*
[13]   Mameli M, Manzoni M, Araneo L, Filippeschi S, Marengo M 2014 Experimental investigation on a closed loop pulsating heat pipe in hyper-gravity conditions *Proc. of the 15th IHTC Conference (Kyoto, Japan, 10-15 Agust 2014)*